Title
Simplified mechanism for new particle formation from methanesulfonic acid, amines, and water via experiments and ab initio calculations

Journal
Proceedings of the National Academy of Sciences, 109(46)

ISSN
0027-8424 1091-6490

Authors
Dawson, M. L
Varner, M. E
Perraud, V.
et al.

Publication Date
2012-10-22

DOI
10.1073/pnas.1211878109

Peer reviewed

Simplified mechanism for new particle formation from methanesulfonic acid, amines, and water via experiments and ab initio calculations

Matthew L. Dawson[a], Mychel E. Varner[a], Véronique Perraud[a], Michael J. Ezell[a], R. Benny Gerber[a,b,c], and Barbara J. Finlayson-Pitts[a,1]

[a]Department of Chemistry, University of California, Irvine, CA 92697-2025; [b]Institute of Chemistry, Fritz Haber Research Center, Hebrew University of Jerusalem, Jerusalem 91904, Israel; and [c]Laboratory of Physical Chemistry, University of Helsinki, FIN-00014 Helsinki, Finland

Edited by* Mark H. Thiemens, University of California San Diego, La Jolla, CA, and approved September 14, 2012 (received for review July 11, 2012)

Airborne particles affect human health and significantly influence visibility and climate. A major fraction of these particles result from the reactions of gaseous precursors to generate low-volatility products such as sulfuric acid and high-molecular weight organics that nucleate to form new particles. Ammonia and, more recently, amines, both of which are ubiquitous in the environment, have also been recognized as important contributors. However, accurately predicting new particle formation in both laboratory systems and in air has been problematic. During the oxidation of organosulfur compounds, gas-phase methanesulfonic acid is formed simultaneously with sulfuric acid, and both are found in particles in coastal regions as well as inland. We show here that: (*i*) Amines form particles on reaction with methanesulfonic acid, (*ii*) water vapor is required, and (*iii*) particle formation can be quantitatively reproduced by a semiempirical kinetics model supported by insights from quantum chemical calculations of likely intermediate clusters. Such an approach may be more broadly applicable in models of outdoor, indoor, and industrial settings where particles are formed, and where accurate modeling is essential for predicting their impact on health, visibility, and climate.

kinetics modeling | multi-component nucleation | cluster enthalpy | flow tube reactor | atmospheric nanoparticles

Understanding how gas phase precursors lead to the formation and growth of new particles that are important for scattering light, for serving as cloud condensation or ice nuclei, and for transport deep into the lung, is one of the most pressing scientific problems (1–5). The most studied system is the conversion of gas-phase SO_2 to sulfuric acid and sulfate particles, but even in this case, models typically underestimate particle formation by an order of magnitude or more (3, 4, 6). However, an accurate predictive capability based on molecular-level understanding is critical for projecting the impacts of particles and developing optimal control strategies.

Classical nucleation theory (CNT) has been used for almost a century (7, 8) to predict new particle formation. At its heart, CNT is a thermodynamics approach that assumes that the precursor clusters have bulk liquid properties such as surface tension, and that addition to and evaporation from the clusters occurs via monomers. Modifications to CNT using kinetics approaches have been described (9, 10). More recently, dynamical nucleation theory (11–13) examined intermolecular interactions and used them to obtain rate constants for the individual steps through variational transition-state theory. This theory has been applied to particle formation in relatively simple systems and clusters of relatively few molecules. Recent data from field and laboratory studies, however, suggest that multicomponent systems with multiple reaction steps are likely involved in new particle formation in the atmosphere (14–22).

We report here a combination of experimental and theoretical studies of new particle formation from mixtures of methanesulfonic acid (MSA), amines, and water. We show that a simple kinetics model based on theoretical calculations of structures of molecular clusters that are likely to play central roles in new particle formation can reproduce the experimentally measured formation of new particles quite well. This approach is promising because it has minimal computational demands, and hence is suitable for inclusion in large-scale models, yet still reflects the basic underlying chemistry.

This particular system was chosen because organosulfur compounds, generated from biological processes in the oceans and from agricultural, industrial, and domestic activities (23–27), form MSA alongside sulfuric acid when oxidized in air (3, 28). Although it is known that ammonia and amines enhance particle formation from sulfuric acid (14–19, 29, 30), the effect of amines on MSA chemistry has not been reported. Their impact on atmospheric particle formation could be important, given that there are many sources of amines in air (31) and gas-phase MSA is typically 10–100% of that of gas-phase H_2SO_4 in the coastal marine boundary layer (32, 33). MSA is commonly detected in atmospheric particles (34–36), and particulate methanesulfonate, dimethylamine (DMA), and cloud condensation nuclei (CCN) activity have been observed to be highly correlated (36). Several field studies have shown enhanced MSA concentrations in small particles when ammonia or amines are present (37, 38), supporting a role for MSA and amines in new particle formation. The impact of MSA and amines on new particle formation may be especially important in the remote marine atmosphere, particularly in polar regions (39–41). However, mechanisms of particle formation in such areas remain unclear.

Results

Flow Tube Experiments. Experiments were performed in an aerosol flow reactor (42) at atmospheric pressure and 25 °C where measured gas-phase MSA, water, and trimethylamine (TMA) or DMA were mixed, and number concentrations of the new particles were determined using a scanning mobility particle sizer (SMPS) whose lower detection limit of 3 nm defined what was measured as a particle and what was modeled using the kinetics scheme discussed below. (Potential effects of particle coagulation and wall losses, discussed in *SI Text*, are shown not to alter the conclusions.)

Fig. 1 shows the number concentrations of new particles formed after 4.2-min reaction time when MSA reacts with water, an amine, or a combination of the two (initial concentrations used

Author contributions: R.B.G. and B.J.F.-P. designed research; M.L.D., M.E.V., V.P., M.J.E., R.B.G., and B.J.F.-P. performed research; M.L.D., M.E.V., V.P., M.J.E., R.B.G., and B.J.F.-P. analyzed data; and M.L.D., M.E.V., V.P., M.J.E., R.B.G., and B.J.F.-P. wrote the paper.

The authors declare no conflict of interest.

*This Direct Submission article had a prearranged editor.

[1]To whom correspondence should be addressed. E-mail: bjfinlay@uci.edu.

This article contains supporting information online at www.pnas.org/lookup/suppl/doi:10.1073/pnas.1211878109/-/DCSupplemental.

ENVIRONMENTAL SCIENCES

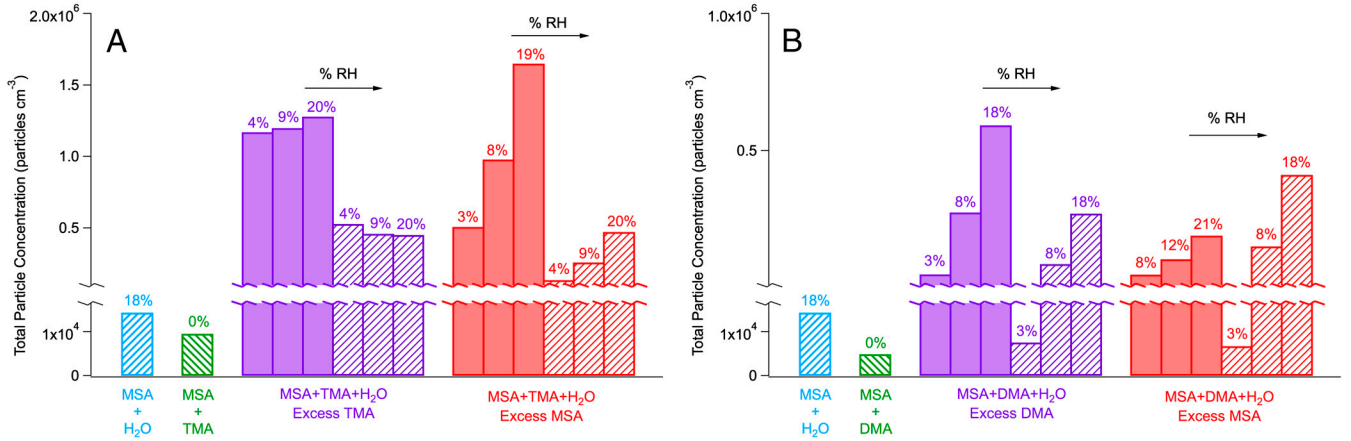

Fig. 1. Total particle concentrations at 4.2-min reaction time for (*A*) TMA and (*B*) DMA with various precursor concentrations and relative humidities. Initial gas-phase concentrations ranged from 2–34 ppb MSA, 0–8 ppb TMA and DMA, and 0–21% RH. Specific experimental conditions are summarized in Table S1.

in these experiments are summarized in Table S1). In agreement with previous studies (43–45), the MSA/water combination does not efficiently form particles compared to sulfuric acid/water. Surprisingly, even mixtures of the strong acid MSA with the basic amines do not lead to significant particle formation; the presence of both the amine and water vapor is required.

The particle number concentrations clearly depend on the concentrations of MSA and the amine. In excess TMA, there is no significant dependence of particle formation on relative humidity (RH), although water is required for particle formation (Fig. 1*A*). However, there is always a dependence on RH in the case of DMA (Fig. 1*B*). In both cases, the number concentration increases with RH in the presence of excess MSA.

Theoretical Calculations. To elucidate the mechanisms of particle formation, quantum chemical calculations were carried out to determine equilibrium structures and enthalpy as well as free energy changes for formation of complexes and small clusters that could lead to particle formation. Structural features of these early-stage species were considered in evaluating their potential for particle formation, particularly "dangling" –NH or –OH groups (Fig. 2) that may be especially efficient in additional hydrogen-bond formation and, we propose, continued particle growth. In addition to the number of hydrogen-bond donor sites, a steric factor was used to consider qualitatively the geometric accessibility of potential hydrogen-bond acceptor sites. A diagram of the enthalpy changes (Fig. 3) for the plausible initial steps was used to ensure that the proposed intermediates are energetically stable. The goal was not to provide an exhaustive list of potential contributing processes, but to use the above criteria to consider feasible routes to particle formation to aid in the development of the kinetics model.

MSA is known to form hydrates in the gas phase (43–45). Although hydrates of amines have also been observed (46, 47), the binding energies for DMA and TMA with water are several kcal mol^{-1} (1 kcal = 4.18 kJ) less than for MSA•H_2O (see Fig. 3 and refs. 48–50). As a result, only reaction of MSA hydrates is included in our simplified reaction scheme. Addition of TMA or DMA to a MSA•H_2O complex (Fig. 2*A*) yields the stable MSA•amine•H_2O cluster (Figs. 2 *B* and *E* and 3). Both clusters have hydrogen-bonding sites that are sterically available for further addition of MSA, amine, or water (Fig. 2 *C* and *F*), all of which are exothermic processes (Fig. 3).

The MSA•amine•H_2O clusters could be expected to lose water reversibly, producing the MSA•amine complexes (Fig. 2 *D* and *G*). Although it is not included in Fig. 3, the entropic contribution to the relative stabilities caused by the vibrational density of states makes this process less unfavorable than it

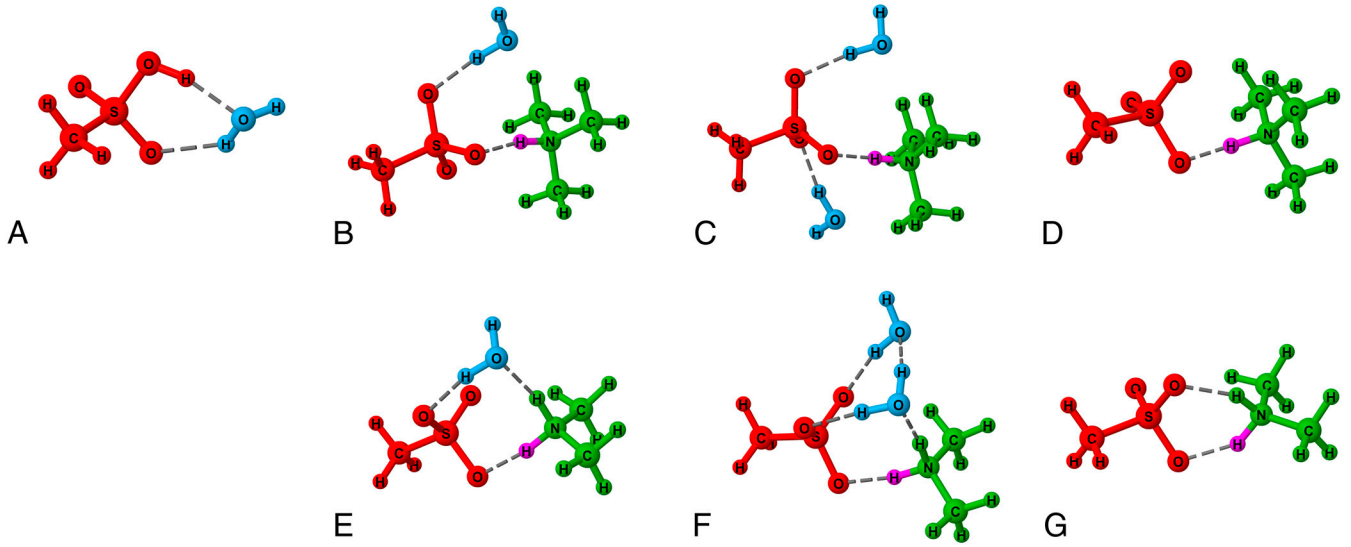

Fig. 2. Structures for (*A*) MSA•H_2O, (*B*) MSA•TMA•H_2O, (*C*) MSA•TMA•$(H_2O)_2$, (*D*) MSA•TMA, (*E*) MSA•DMA•H_2O, (*F*) MSA•DMA•$(H_2O)_2$, and (*G*) MSA•DMA. MSA in red, TMA and DMA in green, H_2O in blue, and transferred proton in pink.

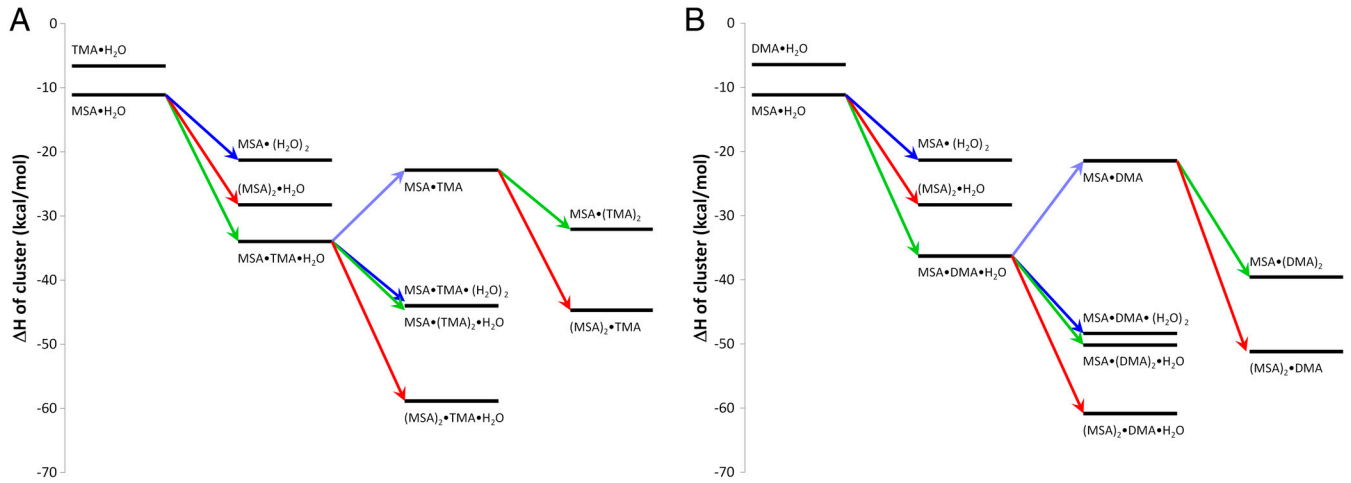

Fig. 3. Calculated change in enthalpy for formation of (*A*) TMA and (*B*) DMA clusters relative to the separated molecules. Arrows indicate addition or loss of MSA (red); TMA or DMA (green); and water (blue).

appears from a strictly energetic perspective. The MSA•amine complexes have accessible hydrogen-bond acceptor sites that make further growth by addition of gas-phase species possible.

Kinetics Model. Fig. 4 summarizes a reaction scheme for this system that treats particle formation as a simple gas-phase kinetics problem. The clusters included in the kinetics model were chosen based on their computed structures, energetics, expected ability to form hydrogen bonds, and the empirical observation that significant new particle formation requires all three gas-phase species.

The model assumes that after the formation of the MSA•H_2O complex, the intermediates that are stable relative to the gas-phase species and have the ability to hydrogen bond to new species play a key role in the formation of new particles. The formation of MSA•H_2O and MSA•amine•H_2O was assumed to be diffusion-controlled. Second-order rate constants (k_1, k_2, and k_{-3}) were calculated (3) according to Eq. **1**:

$$k = \pi(r_i + r_j)^2 \sqrt{\frac{8k_B T}{\pi\mu}}. \qquad [1]$$

Here, μ is the reduced mass of the colliding species, k_B is the Boltzmann constant and T is temperature. Eq. **1** assumes clusters and gas-phase species act as hard spheres of radius r. These radii were estimated from the largest distance between atomic nuclei for the corresponding structures shown in Fig. 2. Although some error is associated with this estimate of cluster size, small changes in the assumed radii have been shown not to affect cluster formation rates significantly (51). The rate constants for the first-order reactions (k_{-1}, k_{-2}, and k_3) were calculated (3) using the forward rate constants and the calculated ΔG values (Table 1). The rate constants k_4 to k_8, which represent overall rate constants

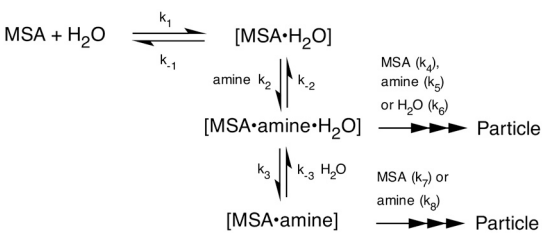

Fig. 4. Proposed reaction scheme for particle formation from the MSA/amine/H_2O system. Species labeled "Particle" are assumed to continue to grow to sizes detectable using our SMPS (≥3 nm).

for the reactions that convert the key intermediates into particles, were adjusted to fit the experimental data.

The ability of this kinetics scheme to describe particle formation in this system was investigated by numerically integrating the rate equations corresponding to the reactions shown in Fig. 4 using a commercially available ordinary differential equations solver, Acuchem (52), for each set of experimental conditions (i.e., initial gas-phase species concentrations). Acuchem uses an integrator that is suitable for "stiff" mathematical equations typical of kinetics problems, and makes use of a user-defined integration tolerance in dynamically determining the integration time step (52). Varying the integration tolerance from the recommended value of 10^{-3} to 10^{-6} resulted in a maximum change in modeled particle concentration of less than 0.2% for all sets of experimental conditions.

Fig. 5 *A* and *B* shows the relationship between laboratory-measured and model-predicted particle concentrations for the TMA and DMA systems, respectively. Error bars were calculated based on ±25% variation in the initial gas-phase concentrations of MSA and the amine to give an indication of the dependence of the modeled results on precursor concentrations.

Table 1. Rate constants* used to model nucleation from MSA/TMA/H_2O and MSA/DMA/H_2O systems using Fig. 4 reaction scheme and ΔG values under standard conditions

	TMA	ΔG (kcal mol^{-1})		DMA	ΔG (kcal mol^{-1})
k_1	6.58 (−10)†		k_1	6.58 (−10)†	
k_{-1}	5.53 (8)‡	2.0§	k_{-1}	5.53 (8)‡	2.0§
k_2	1.32 (−9)†		k_2	1.44 (−9)†	
k_{-2}	3.09 (1)‡	12.3§	k_{-2}	5.29 (0)‡	13.4§
k_3	9.96 (8)‡	2.2§	k_3	7.91 (6)‡	5.0§
k_{-3}	1.66 (−9)†		k_{-3}	1.49 (−9)†	
k_4	6.00 (−19)		k_4	3.00 (−20)	
k_5	5.00 (−19)		k_5	1.00 (−20)	
k_6	2.00 (−25)		k_6	3.00 (−25)	
k_7	5.00 (−20)		k_7	1.00 (−20)	
k_8	4.00 (−19)		k_8	7.00 (−20)	

*First-order rate constants in units of s^{-1} and second-order rate constants in units of cm^3 $molecules^{-1}$ s^{-1}. Also, $1.65\ (-10) = 1.65 \cdot 10^{-10}$.

†Assumed to be diffusion-controlled and calculated using hard-sphere collision theory with activation energies of zero.

‡Calculated from ΔG of formation for intermediates, the relationship between ΔG and the equilibrium constant and the value of the forward rate constant.

§Positive values indicate that loss of water from MSA•H_2O (k_{-1}) and MSA•amine•H_2O (k_3) and loss of amine from MSA•amine•H_2O (k_{-2}) are endoergic.

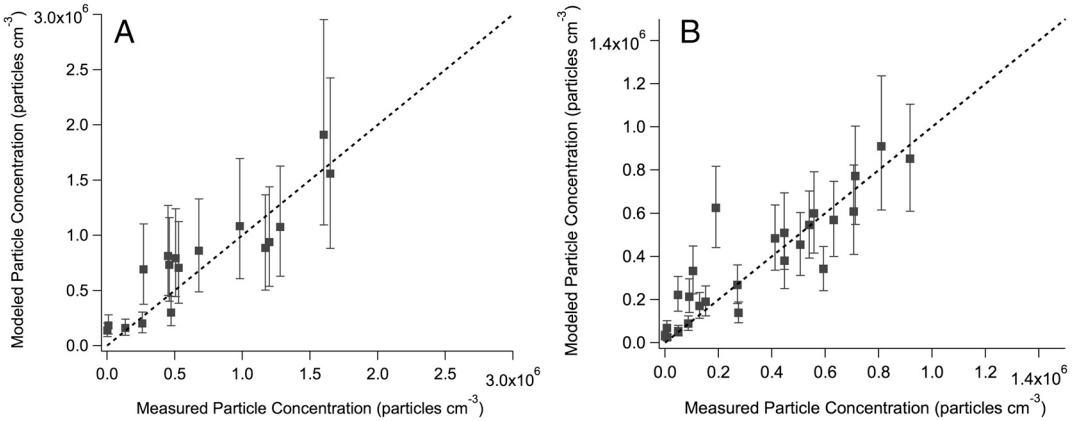

Fig. 5. Comparison of n modeled and measured particle concentrations at 4.2-min reaction time for the reaction of MSA, H_2O, and (*A*) TMA ($n = 17$) and (*B*) DMA ($n = 25$). Rate constants are presented in Table 1. The dashed line has a slope of 1 and is included for reference. Error bars indicate changes in modeled particle concentration with ±25% of the initial gas-phase MSA and amine concentrations.

Discussion

As evident from Fig. 5, the model is able to reproduce the new particle concentrations for both TMA and DMA over a range of conditions quite well, supporting this type of mechanistic approach for new particle formation in multicomponent atmospheric systems.

A key finding is the need for water to form new particles, despite the fact that MSA/water alone does not form particles efficiently, as reported in earlier studies (43–45). A strong acid like MSA must react rapidly with amines, yet interestingly, this also does not lead to significant new particle formation (Fig. 1). Water clusters to the amines and MSA in such a way that hydrogen-bonding sites are readily available from a steric point of view (Fig. 2). Such structures permit the addition of more species from the gas phase, eventually forming particles. This is an intriguing role for water, which has been shown to be important in a number of different atmospherically relevant reactions (53).

The requirement for water arises from two sources: (*i*) the central role of the MSA hydrate as a particle precursor; and (*ii*) the reaction of the MSA•amine•H_2O complex with water, reaction 6, to form particles. The major difference experimentally between DMA and TMA is for the case of excess amine, where, surprisingly, the number of new particles formed from TMA does not increase with RH (although water vapor is required; Fig. 1). DMA, however, does have a dependence on RH. The difference is rooted in the structures and calculated free energy differences between the MSA•amine•H_2O and MSA•amine complexes (Fig. 2 and Table 1). For the TMA case, $\Delta G = +2.2$ kcal mol^{-1} for conversion of MSA•amine•H_2O to the MSA•amine complex, whereas for DMA, $\Delta G = +5.0$ kcal mol^{-1} under standard conditions (Table 1). Thus the MSA•amine intermediate contributes to new particle formation for TMA, whereas for DMA, MSA•amine•H_2O is more important. This shunts more of the chemistry through the MSA•amine complex for TMA, and under conditions of excess TMA, reaction 8 becomes the dominant source of particles. Although TMA cannot hydrogen bond to the MSA•TMA complex, it is predicted to form a stable MSA•$(TMA)_2$ cluster (Fig. 3*A*). Because water vapor is in great excess, the reaction is limited by the amount of MSA, which is completely titrated by the excess TMA in forming the MSA•TMA•H_2O complex. As a result, there is little increase in new particle formation with increasing RH, although water is required because the MSA hydrate is the reactive precursor. In the case of DMA, particle formation occurs primarily through the MSA•amine•H_2O complex where the reaction with a second water molecule gives an additional water vapor dependence.

Interpretation of the experimental data in terms of classical nucleation theory is complicated by the multicomponent and multistep nature of the system. Detailed kinetics mechanisms have been used to describe cluster and particle formation in other systems, including those formed from sulfuric acid, water, and ammonia or amines (51, 54, 55), but without a direct comparison to experimental data. The approach presented here is based on an integration of quantum chemical calculations with experimental data and kinetics modeling. It provides a framework for incorporating new particle formation into atmospheric models in a relatively straightforward, semiempirical manner with minimal computational cost that still reflects the fundamental molecular interactions that are key to the process.

In several field studies in marine areas, the concentration of MSA in the smallest particles was similar to that of non-sea salt sulfate (37, 38). This suggests that in coastal areas, MSA can contribute to new particle formation at levels similar to that of sulfuric acid. The results presented here are consistent with these field observations. Gas-phase sulfuric acid concentrations in air are typically in the range of 10^5 to 10^7 molecules cm^{-3} in both marine and midcontinental regions (33, 56), and MSA is approximately 10–100% of that of H_2SO_4 (32, 33). Amine concentrations in air are not well-known, particularly for coastal areas, but for rural areas, total amine concentrations of a few tens to hundreds of parts per trillion (ppt) have been reported (31). Close to sources, the concentrations can be parts per billion (ppb) or greater (31). Facchini et al. (38) show that amines are found in marine particles with MSA and propose that there is a marine source of gas-phase amines. The kinetics model was run with MSA at 10^6 molecules cm^{-3}, TMA or DMA at 500 ppt, and RH of 30%. Under these conditions, particles are predicted to be formed at rates of approximately 0.004–0.02 particles cm^{-3} s^{-1} for TMA and DMA, respectively. For comparison, using the parameterization of field measurement data of Kuang et al. (57) that was collected under a variety of conditions (which would include the presence of ammonia and amines), sulfuric acid at 10^6 molecules cm^{-3} forms particles at a rate of 0.01–10 particles cm^{-3} s^{-1}. Thus our model predicts that under some atmospheric conditions, particle formation from MSA should be similar in magnitude to that from sulfuric acid, as indicated by the field measurements (37, 38). It is noteworthy that this consistency between the model predictions and field results arises even though atmospheric concentrations of MSA are typically ppt (28, 32), as assumed in the model calculations, rather than ppb, which is experimentally accessible in our system. Once new particles have been formed from MSA, they can then grow by uptake of low and semivolatile gases formed in other atmospheric processes.

In summary, our experiments clearly show that MSA and amines form particles and that water plays a key role in the process. Using theoretical calculations of possible important

intermediates to guide the development of a relatively simple mechanistic scheme gave good agreement with the experimentally measured dependence of new particle formation on the concentrations of the precursors in this complex, multicomponent system. Although the specific case described here involves MSA and amines, the role of water and the kinetics formulation based on the structures and thermodynamics of key intermediates integrated with experimental data are expected to be applicable in other important multicomponent systems, such as sulfuric or organic acids with amines. (Indeed, an analogous approach recently applied to atmospheric field measurements was much more successful than traditional analyses for predicting new particle formation from sulfuric acid in air; see ref. 22.) It is noteworthy that our results suggest that rates of new particle formation can be a complex function of not only the nature and concentration of the precursors, including water, but also which precursor specifically is the "limiting reagent." This approach may be broadly useful for calculating new particle formation wherever it occurs, including outdoors, indoors, and in industrial settings.

Materials and Methods

Gas-phase DMA (1.4 ppm in N_2; Airgas) or TMA (13.4 ppm in N_2; Matheson) was introduced into the aerosol flow reactor (University of California, Irvine) (42) in a stream of 40 Lpm dry compressed air purified by passing through a purge gas generator (Model 75-62; Parker Balston), carbon/alumina media (Perma Pure, LLC), and a 0.1-μm filter (DIF-N70; Headline Filters). In experiments with RH > 0%, some of the air stream was diverted through a humidifier (Model FC125-240-5MP; Perma Pure, LLC) before entering the flow reactor to achieve the desired RH. Downstream of the amine/water vapor inlet, at a distance corresponding to a mixing time of 4.3 min, gas-phase MSA was introduced into the flow reactor, and then, after an additional 4.2-min reaction time, particles were sampled. The gas-phase MSA was generated by flowing dry purified air over pure liquid MSA (99.0%; Aldrich). The gas-phase concentration of MSA in the flow reactor was varied by adjusting the flow of air over the liquid MSA from 1.5 to 3.0 Lpm.

Gas-phase MSA concentrations were measured by sampling from the flow reactor for 30 min at 1 Lpm onto 25-mm by 0.45-μm Durapore filters (Millex-HV) followed by extraction in Nano-Pure water (Model 7146; Thermo Scientific) and analysis by ultraperformance liquid chromatography MS (Waters). The filter collection method of measuring gas-phase MSA concentrations used in these experiments was tested by collection using two filters in series, and by performing two extractions on a single filter. No MSA was detected on the second inline filter or in the second extraction of a filter sample, even at approximately 10–50 times higher MSA concentrations than were used in the flow tube experiments. Measurement of three replicate samples gave a 2*s* error of 20% for the MSA concentration (*s* is the sample standard deviation defined as $s = \sqrt{\frac{\sum (x-a)^2}{(N-1)}}$, where N is the number of samples, x is the measured concentration, and a is the average of all measured concentrations). Gas-phase DMA and TMA concentrations were calculated using the flow rates and the known concentrations in the gas cylinders. Particle size distributions were measured with a SMPS consisting of a classifier (Model 3080; TSI), a differential mobility analyzer (Model 3081; TSI), and a condensation particle counter (Model 3776; TSI).

Structures of potential intermediate clusters were optimized using the hybrid density functional B3LYP supplemented with Grimme's semiempirical dispersion correction (58) and using the 6–31++G(*d, p*) basis set. The hybrid functional, dispersion correction, and basis set with diffuse functions were used in this study of ion pair clusters to avoid potential self-interaction error and to properly treat long-range interactions (59). Harmonic frequency calculations were carried out for calculation of the thermal component of the enthalpy at standard conditions. The electronic energy component of the enthalpy was calculated at the resolution of the identity–second-order Møller–Plesset (RI-MP2)/aug-cc-$pV(T+d)Z$ level of theory. The lowest-energy isomer of each cluster was identified, and the enthalpies of reaction to form clusters from the gas-phase species were used to construct Fig. 3. The low-energy isomers of the species included in the kinetic model were also optimized and harmonic frequencies calculated at the RI-MP2/aug-cc-$pV(D+d)Z$ level of theory and the RI-MP2/aug-cc-$pV(T+d)Z$ energy was determined at the new geometry. The differences in the enthalpies and free energies calculated using the DFT and MP2 approaches were less than 1 kcal mol^{-1} and typically less than 0.5 kcal mol^{-1}. Ortega et al. (55) tested several approaches for calculating the enthalpy and Gibbs free energies for clusters of sulfuric acid and ammonia. The Gibbs free energy and enthalpy, −7.61 kcal mol^{-1} and −16.0 kcal mol^{-1} (calculated for the sulfuric acid and ammonia complex using their chosen method), respectively, are very similar to the results for the MP2 approach used here: −7.51 kcal mol^{-1} and −15.8 kcal mol^{-1}. The calculated enthalpies for formation of the TMA•H_2O complex, −6.7 kcal mol^{-1} with B3LYP-D/6–31++G(*d, p*) and −6.8 kcal mol^{-1} with RI-MP2/aug-cc-$pV(D+d)Z$, compare well with the experimental value $-6.91 +/- 0.05$ kcal mol^{-1} (46).

The rate equations involved in the kinetics scheme described in Fig. 4 were numerically integrated using Acuchem (52) for each set of experimental conditions. The structure, harmonic frequency, and free energy calculations were carried out using the TURBOMOLE v. 6.3 (60) program package.

ACKNOWLEDGMENTS. We thank James N. Pitts, Jr., and Michael Prather for helpful discussions, and John Greaves for assistance with the MSA analysis. This work was performed under Department of Energy Grant DE-SC0006606 and National Science Foundation Grant 0909227, with computational resources provided through National Science Foundation Grant CHE-0840513. R.B.G. acknowledges partial support by Israel Science Foundation Grant 114/08.

1. Pauchauri RK, Reisinger A, eds., and Intergovernmental Panel on Climate Change (2007) Climate change 2007: Synthesis report. Contribution of working groups I, II and III to the fourth assessment report of the intergovernmental panel on climate change. *The IPCC 4th Assessment Report* (IPCC, Geneva), Core Writing Team.
2. Pope CA, III, Dockery DW (2006) Health effects of fine particulate air pollution: Lines that connect. *J Air Waste Manag Assoc* 56:709–742.
3. Finlayson-Pitts BJ, Pitts JN, Jr (2000) *Chemistry of the Upper and Lower Atmosphere—Theory Experiments and Applications* (Academic Press, San Diego).
4. Seinfeld JH, Pandis SN (2006) *Atmospheric Chemistry and Physics: From Air Pollution to Climate Change* (Wiley Interscience, New York).
5. Phalen RF (1984) *Inhalation Studies: Foundations and Techniques* (CRC, Boca Raton, FL).
6. Sipila M, et al. (2010) The role of sulfuric acid in atmospheric nucleation. *Science* 327:1243–1246.
7. Kashchiev D (2000) *Nucleation: Basic Theory with Applications* (Butterworth, Oxford).
8. Vehkamaki H (2006) *Classical Nucleation Theory in Multicomponent Systems* (Springer, Berlin).
9. Girshick SL (1997) Theory of nucleation from the gas phase by a sequence of reversible reactions. *J Chem Phys* 107:1948–1952.
10. McGraw R, Wu DT (2003) Kinetic extensions of the nucleation theorem. *J Chem Phys* 118:9337–9347.
11. Kathmann SM, Schenter GK, Garrett BC, Chen B, Siepmann JI (2009) Thermodynamics and kinetics of nanoclusters controlling gas-to-particle nucleation. *J Phys Chem C* 113:10354–10370.
12. Kathmann SM, Schenter GK, Garrett BC (2008) The impact of molecular interactions on atmospheric aerosol radiative forcing. *Adv Quant Chem* 55:429–447.
13. Devarajan A, Windus TL, Gordon MS (2012) Implementation of dynamical nucleation theory effective fragment potentials method for modeling aerosol chemistry. *J Phys Chem A* 115:13987–13996.
14. Angelino S, Suess DT, Prather KA (2001) Formation of aerosol particles from reactions of secondary and tertiary alkylamines: Characterization by aerosol time-of-flight mass spectrometry. *Environ Sci Tech* 35:3130–3138.
15. Berndt T, et al. (2010) Laboratory study on new particle formation from the reaction $OH + SO_2$: Influence of experimental conditions, H_2O vapor, NH_3, and the amine tert-butylamine on the overall process. *Atmos Chem Phys* 10:7101–7116.
16. Kirkby J, et al. (2011) Role of sulphuric acid, ammonia and galactic cosmic rays in atmospheric aerosol nucleation. *Nature* 476:429–477.
17. Smith JN, et al. (2010) Observations of aminium salt formation in atmospheric nanoparticles: Implications for aerosol growth. *Proc Natl Acad Sci USA* 107:6634–6639.
18. Yu H, McGraw R, Lee S-H (2012) Effects of amines on formation of sub-3 nm particles and their subsequent growth. *Geophys Res Lett* 39, 10.1029/2011GL050099.
19. Zollner JJ, et al. (2012) Sulfuric acid nucleation: Power dependencies, variation with relative humidity and effect of bases. *Atmos Chem Phys* 12:4399–4411.
20. Metzger A, et al. (2010) Evidence for the role of organics in aerosol particle formation under atmospheric conditions. *Proc Natl Acad Sci USA* 107:6646–6651.
21. Zhang R, et al. (2004) Atmospheric new particle formation enhanced by organic acids. *Science* 304:1487–1490.
22. Chen M, et al. (2012) An acid-base chemical reaction model for nucleation rates in the polluted atmospheric boundary layer. *Proc Natl Acad Sci USA*, in press.
23. Bates TS, Lamb BK, Guenther A, Dignon J, Stoiber RE (1992) Sulfur emissions to the atmosphere from natural sources. *J Atmos Chem* 14:315–337.
24. Kettle AJ, et al. (2001) Assessing the flux of different volatile sulfur gases from the ocean to the atmosphere. *J Geophys Res* 106:12193–12209.
25. Kim KH (2006) Emissions of reduced sulfur compounds (RSC) as a landfill gas (LFG): A comparative study of young and old landfill facilities. *Atmos Environ* 40:6567–6578.
26. Lamb B, Westberg H, Allwine G, Bamesberger L, Guenther A (1987) Measurement of biogenic sulfur emissions from soils and vegetation: Application of dynamic enclosure methods with Natusch filter and GC/FPD analysis. *J Atmos Chem* 5:469–491.

27. Trabue S, et al. (2008) Field sampling method for quantifying volatile sulfur compounds from animal feeding operations. *Atmos Environ* 42:3332–3341.
28. Mauldin RL, III, Tanner DJ, Heath JA, Huebert BJ, Eisele FL (1999) Observations of H_2SO_4 and MSA during PEM-Tropics-A. *J Geophys Res* 104:5801–5816.
29. Loukonen V, et al. (2010) Enhancing effect of dimethylamine in sulfuric acid nucleation in the presence of water: A computational study. *Atmos Chem Phys* 10:4961–4974.
30. Kurtén T, Loukonen V, Vehkamäki H, Kulmala M (2008) Amines are likely to enhance neutral and ion-induced sulfuric acid-water nucleation in the atmosphere more effectively than ammonia. *Atmos Chem Phys* 8:4095–4103.
31. Ge X, Wexler AS, Clegg SL (2010) Atmospheric amines. Part I. A Review. *Atmos Environ* 45:534–546.
32. Berresheim H, et al. (2002) Gas-aerosol relationships of H_2SO_4, MSA, and OH: Observations in the coastal marine boundary layer at Mace Head, Ireland. *J Geophys Res* 107, doi:10.1029/2000JD000229.
33. Eisele FL, Tanner DJ (1993) Measurement of the gas phase concentration of H_2SO_4 and methane sulfonic acid and estimates of H_2SO_4 production and loss in the atmosphere. *J Geophys Res* 98:9001–9010.
34. Gaston CJ, Pratt KA, Qin XY, Prather KA (2010) Real-time detection and mixing state of methanesulfonate in single particles at an inland urban location during a phytoplankton bloom. *Environ Sci Technol* 44:1566–1572.
35. Hopkins RJ, et al. (2008) Chemical speciation of sulfur in marine cloud droplets and particles: Analysis of individual particles from the marine boundary layer over the California current. *J Geophys Res* 113, doi:10.1029/2007JD008954.
36. Sorooshian A, et al. (2009) On the link between ocean biota emissions, aerosol, and maritime clouds: Airborne, ground, and satellite measurements off the coast of California. *Global Biogeochem Cycle* 23, doi:10.1029/2009GB003464.
37. Kerminen VM, Aurela M, Hillamo RE, Virkkula A (1997) Formation of particulate MSA: Deductions from size distribution measurements in the Finnish Arctic. *Tellus Ser B* 49:159–171.
38. Facchini MC, et al. (2008) Important source of marine secondary organic aerosol from biogenic amines. *Environ Sci Technol* 42:9116–9121.
39. Chang RYW, et al. (2011) Relating atmospheric and oceanic DMS levels to particle nucleation events in the Canadian Arctic. *J Geophys Res* 116, 10.1029/2011JD015926.
40. Karl M, Gross A, Leck C, Pirjola L (2007) Intercomparison of dimethylsulfide oxidation mechanisms for the marine boundary layer: Gaseous and particulate sulfur constituents. *J Geophys Res* 112, 10.1029/2006JD007914.
41. Karl M, Leck C, Gross A, Pirjola L (2012) A study of new particle formation in the marine boundary layer over the central Arctic Ocean using a flexible multicomponent aerosol dynamic model. *Tellus B* 64:17158.
42. Ezell MJ, et al. (2010) A new aerosol flow system for photochemical and thermal studies of tropospheric aerosols. *Aerosol Sci Technol* 44:329–338.
43. Kreidenweis SM, Flagan RC, Seinfeld JH, Okuyama K (1989) Binary nucleation of methanesulfonic-acid and water. *J Aerosol Sci* 20:585–607.
44. Wyslouzil BE, Seinfeld JH, Flagan RC, Okuyama K (1991) Binary nucleation in acid water systems. 2. Sulfuric acid-water and a comparison with methanesulfonic acid-water. *J Chem Phys* 94:6842–6850.
45. Wyslouzil BE, Seinfeld JH, Flagan RC, Okuyama K (1991) Binary nucleation in acid water systems. 1. Methanesulfonic acid-water. *J Chem Phys* 94:6827–6841.
46. Millen DJ, Mines GW (1977) Hydrogen bonding in the gas phase. Part 5. Infrared spectroscopic investigation of O–H…N complexes formed by water: Ammonia monohydrate and amine and pyridine monohydrates. *J Chem Soc Faraday Trans 2* 73:369–377.
47. Rozenberg M, Loewenschuss A, Nielsen CJ (2012) H-bonded clusters in the trimethylamine/water system: A matrix isolation and computational study. *J Phys Chem A* 116:4089–4096.
48. Mmereki BT, Donaldson DJ (2002) Ab initio and density functional study of complexes between the methylamines and water. *J Phys Chem A* 106:3185–3190.
49. Wang LM (2007) Clusters of hydrated methane sulfonic acid $CH_3SO_3H\bullet(H_2O)_n$ ($n = 1$–5): A theoretical study. *J Phys Chem A* 111:3642–3651.
50. Givan A, Loewenschuss A (2005) Infrared spectrum and ab initio calculations of matrix isolated methanesulfonic acid species and its 1:1 water complex. *J Mol Struct* 748:77–90.
51. McGrath MJ, et al. (2012) Atmospheric cluster dynamics code: A flexible method for solution of the birth-death equations. *Atmos Chem Phys* 12:2345–2355.
52. Braun W, Herron JT, Kahaner DK (1988) ACUCHEM: A computer program for modeling complex chemical reaction systems. *Int J Chem Kinet* 20:51–62.
53. Vaida V (2011) Perspective: Water cluster mediated atmospheric chemistry. *J Chem Phys* 135:020901.
54. Kulmala M (2010) Dynamical atmospheric cluster model. *Atmos Res* 98:201–206.
55. Ortega IK, et al. (2012) From quantum chemical formation free energies to evaporation rates. *Atmos Chem Phys* 12:225–235.
56. Erupe ME, et al. (2010) Correlation of aerosol nucleation rate with sulfuric acid and ammonia in Kent, Ohio: An atmospheric observation. *J Geophys Res* 115:D23216.
57. Kuang C, McMurry PH, McCormick AV, Eisele FL (2008) Dependence of nucleation rates on sulfuric acid vapor concentration in diverse atmospheric locations. *J Geophys Res* 113:D10209.
58. Grimme S (2006) Semi-empirical GGA-type density functional constructed with a long-range dispersion correction. *J Comput Chem* 27:1787–1799.
59. Grimme S, Hujo W, Kirchner B (2012) Performance of dispersion-corrected density functional theory for the interactions in ionic liquids. *Phys Chem Chem Phys* 14:4875–4883.
60. Ahlrichs R, et al. TURBOMOLE (TURBOMOLE GmbH, Karlsruhe, Germany), Version 6. 3., Available at http://www.turbomole.com.